

FREEZE-THAWING SINGLE HUMAN EMBRYONIC STEM CELLS INDUCE E-CADHERIN AND ACTIN FILAMENT NETWORK DISRUPTION VIA G13 SIGNALING

Hinako Ichikawa¹, Susumu Yoshie¹, Sakiko Shirasawa², Tadayuki Yokoyama²,
Fengming Yue¹, Daihachiro Tomotsune¹, and Katsunori Sasaki^{1*}

¹Department of Histology and Embryology, Shinshu University School of Medicine, 3-1-1
Asahi, Matsumoto, Nagano 390-8621, Japan

²Bourbon Corporation, 4-2-14 Matusnami, Kashiwazaki, Niigata 945-8611, Japan,
Department of Histology and Embryology, Shinshu University School of Medicine, 3-1-1
Asahi, Matsumoto 390-8621, Japan

Phone: +81-263-37-2590, Fax: +81-263-37-3093,

*Corresponding author e-mail: katsmd@shinshu-u.ac.jp

Abstract

Poor adhesion of single human embryonic stem (hES) cells after freeze-thawing causes death. To investigate mechanisms responsible for this, Rho-dependent protein kinase (ROCK) inhibitor Y-27632-treated and untreated single hES cells were analyzed for E-cadherin and F-actin distribution by immunostaining and phalloidin staining respectively and for G13 signaling pathway components by DNA microarray and quantitative polymerase chain reaction (PCR). Y-27632-treated cells clustered rapidly and maintained E-cadherin and F-actin distribution without losing Oct3/4. Immediately after thawing, E-cadherin in untreated hES cells dotted along the membrane and then displayed eccentric cytoplasmic localization. Bleb formation and early Oct3/4 loss occurred after F-actin network condensation in the cytoplasm. Microarray analyses and quantitative PCR indicated upregulation of two actin reorganization-associated components of the G13 signaling pathway, Arhgdib and Cdc42, in untreated cells. Considering these findings and that cell death was partly interrupted by Y-27632, E-cadherin and actin cytoskeleton network disruption through the G13 signaling pathway may cause hES cell death after freeze-thawing.

Keywords: Cryopreservation, E-cadherin, actin filaments, G13 signaling pathway, human embryonic stem cells, ROCK inhibitor

INTRODUCTION

It is well known that human embryonic stem (hES) cells are vulnerable to conventional slow freezing. Their survival rate after thawing is about 1% (19). hES cells cannot live without forming colonies because they have a uniquely intimate co-operative nature (6). The low survival rate is due to destruction of this co-operative nature after freeze-thawing. To solve this serious problem, novel cryoprotocols using the Rho-dependent protein kinase (ROCK) inhibitor Y-27632 were proposed in 2008 (10, 14). This inhibitor protects

dissociated individual hES cells from cell death (23), making it possible to freeze single cells. Similar to mouse ES cells (20), a high survival rate is expected in single hES cells are frozen after treatment with Y-27632. In fact, 70%–80% of such cells are viable immediately after thawing, and 15% form colonies after 10 days of culture (unpublished data under submission). Some studies have attributed this protective effect to suppression of apoptosis (6, 21). Although it is clear that apoptosis plays a major role in promoting cell death, some novel observations have been noted; for example, if individual cells adhere to each other, they survive (9). However, if apoptosis predicted cell death, then this would not be possible. It is difficult to explain that cell death always occurs via apoptosis, and the promotion of the re-adhesion mechanism may be superior to suppression of apoptosis.

Re-adhesion is not regulated by adhesion molecules alone, and the cytoskeletal network, especially actin filaments, plays a major role. Actin filaments are closely associated with the intramembranous adhesion molecule E-cadherin; they regulate E-cadherin distribution via the actin anchor protein and form intercellular junctions (15). Although RhoA and its components are associated with re-adhesion, because activated RhoA induces pathologic hyperactivity of actin filaments (13), possible alterations in E-cadherin distribution and actin filament network as well as molecular mechanisms that accelerate these processes after freeze-thawing remain unknown.

This paper focuses on factors leading to morphological and molecular disruption of the actin filament–E-cadherin association after freeze-thawing and shows that this process triggers cell death; however this cell death is interrupted by the ROCK inhibitor Y-27632.

MATERIALS AND METHODS

Culture of hES cells

KhES-1 cells were supplied by the Institute for Frontier Medical Science, Kyoto University, Japan, (19) and were used in accordance with the hES cell research guidelines established by the Japanese government. The cells were cultured on a feeder layer of mouse embryonic feeder (MEF) cells in a mixture of Dulbecco's modified Eagle's medium and Ham's F12 medium (Nissui Pharmaceutical Co., Ibaraki, Japan) supplemented with 20% (v/v) Knockout Serum Replacement (KSR; Invitrogen, Carlsbad, CA, USA), 2 mM L-glutamine (Invitrogen), 0.1 mM nonessential amino acids (Invitrogen), and 0.1 mM 2-mercaptoethanol (Sigma-Aldrich Co., St. Louis, MO, USA) under a 3% CO₂ atmosphere. For routine passage, hES cell colonies were dispersed gently after treatment with 0.25% trypsin and 0.1 mg/mL collagenase IV (Invitrogen) in phosphate-buffered saline (PBS) containing 20% KSR and 1 mM CaCl₂ at 37°C for 5 min; they were gently pipetted into the medium (19). The clumps were seeded on a dish with a new feeder layer.

Cryopreservation of dissociated hES cells and experimental design

First, hES cell colonies were detached from MEF cells using the above dispersion cocktail and were partially dissociated as clumps. Next, contaminated MEF cells were removed by incubating the cell suspension on a gelatin-coated plate at 37°C for 1 h in culture medium, and they rapidly adhered to the plastic dish. The remaining hES cell clumps were separated from the suspension by centrifugation, incubated in 0.1% (v/v) trypsin–ethylenediaminetetraacetic acid (Invitrogen) at 37°C for 4 min, pipetted into the conditioned medium containing 10 μM Y-27632 or left untreated, dissociated completely into single cells, centrifuged, diluted with the medium, and then passed through a 40-μm cell strainer (BD Falcon, New Jersey, USA). The dissociated cells in the designed medium were centrifuged, diluted with 1 mL of the freezing medium consisting of hES cell culture medium with 10% dimethylsulfoxide (Sigma-Aldrich Co.), transferred to cryovials (Nalgene Cryogenic Vials,

Nalge Nunc, NY, USA) and frozen slowly in a Bicell container (Nihon Freezer, Tokyo, Japan) at -80°C overnight. The cooling rate of the Bicell was identical to that described previously (8). The cells were then stored in liquid nitrogen for more than a week before being rapidly thawed in a water bath at 37°C . To investigate the effect of the ROCK inhibitor on cryopreserved dissociated hES cells, the following experiment was performed. After thawing, $10\ \mu\text{M}$ Y-27632 was added to both the freezing medium and the culture medium of R_i (ROCK inhibitor) (+) cells for 1 day and was not added to any medium for R_i (-) cells.

Immunostaining

hES colonies and dissociated hES cells were fixed with 4% paraformaldehyde (PFA) in 0.1 M phosphate buffer (pH 7.4) for 1 h at room temperature and then rinsed three times with 20 mM PBS (pH 7.4). Before immunostaining, specimens were treated with 0.5% Triton X-100/20 mM PBS for 30 min for permeabilization and rinsed three times in 20 mM PBS. Treated cells were stained with antibodies against E-cadherin (rabbit polyclonal, Santa Cruz, CA, USA) and Oct3/4 (mouse monoclonal, Santa Cruz).

Following application of the primary antibodies, specimens were incubated with a mixture of appropriate secondary antibodies conjugated to Alexa Fluor 488/568 and 4',6-diamino-2-phenylindole dihydrochloride (DAPI; Molecular Probes, Eugene, OR, USA). The specimens were observed under a Zeiss Axio Observer Z1 microscope (Carl Zeiss, Jena, Germany).

F-actin staining

hES cells were fixed with 4% PFA, permeabilized with 0.1% Triton X-100, and blocked with 1% bovine serum albumin (BSA) in PBS. F-actin staining dye, Texas Red-X phalloidin (Invitrogen), was applied for 30 min at room temperature. After washing with PBS, nuclear counter staining (DAPI) was performed for 5 min. The specimens were observed under a ZEISS Axio Observer Z1 microscope.

Some components of the G13 signaling pathway detected by DNA microarray

To investigate the effects of Y-27632 on the G13 signaling pathway in cryopreserved individual hES cells, we screened some components of the pathway by DNA microarray. Total RNA from R_i (+) and R_i (-) cells was extracted using the TRIzol Reagent (Invitrogen) according to the manufacturer's instructions. RNA ($1\ \mu\text{g}$) was transcribed into double-stranded T7 RNA polymerase promoter-tagged cDNA and then amplified into single-stranded biotin-labeled cRNA using T7 polymerase (22). Aliquots ($3\ \mu\text{g}$) of cRNA were fragmented at 94°C for 15 min and hybridized on a Conpath[®] chip (GEO ID GPL 5366, DNA Chip Research Inc., Yokohama, Kanagawa, Japan) in the presence of formamide at a final concentration of 10% v/v at 37°C for 16 h. After washing, the chip was immersed in a NaCl/ P_i solution containing $10\ \mu\text{g}/\text{mL}$ streptavidin/R-phycoerythrin conjugate (Invitrogen), Tween-20 (0.05% v/v), and BSA ($2\ \text{mg}/\text{mL}$) for 30 min and then rinsed in $0.05\times$ saline-sodium citrate buffer before drying by low-speed centrifugation. The chip was scanned using the Agilent DNA microarray scanner (Agilent Technologies, Santa Clara, CA, USA) at a resolution of $10\ \mu\text{m}$ (photomultiplier tube: 80). The intensity values of each feature of the scanned image were quantified using Feature Extraction software (version 9.1, Agilent Technologies), which performed background subtractions. Features that were flagged according to the software algorithm or those below the background value were excluded from further analysis. Normalization was performed using GeneSpring GX version 7.31 (Agilent Technologies). Each chip was normalized to the 50th percentile, and each gene was normalized to the control reference sample R_i (+). Expression ratios were calculated for features that were present in both reference and tested samples. The microarray data was

deposited to NCBI GEO with accession number GSE21796, (<http://www.ncbi.nlm.nih.gov/geo/query/acc.cgi?acc=GSE21796>) and some components of the G13 pathway were screened using human gene information data (Hs-Std_20060526.gdb) and human pathway data (Hs_Contributed_20070308) provided by the Gene Map Annotator and Pathway Profile (GenMAPP) (<http://www.genmapp.org>) (2,3).

Quantitative reverse transcription-polymerase chain reaction (PCR)

Candidate components screened with microarray were confirmed by quantitative PCR. Total RNA was extracted from cells using the TRIzol Reagent (Invitrogen) according to the manufacturer's instructions. First-strand cDNA was synthesized from 1 µg of total RNA using the PrimeScript RT reagent kit (Takara Bio, Otsu, Japan). Quantitative PCR analysis was performed for two components of the G13 pathway, *Arhgdib* and *Cdc42*, which were shown to be upregulated by a previous microarray analysis, and *β-actin* using a Thermal Cycler Dice Real-Time System (Takara Bio). The PCR amplification reaction mix consisted of 12.5 µL SYBR Green PCR Master Mix (Takara Bio), 0.5 µL of 0.2 µM forward and reverse primers, 1 µL of 100 ng/µL template cDNA, and 10.5 µL distilled water in a total volume of 25 µL. Cycling was performed for 10 min at 95°C, followed by 40 cycles at 95°C for 5 s and 60°C for 30 s, which were the default conditions of the Thermal Cycler Dice Real-Time System software TP 800 (version 2.0). The primer sets for *β-actin*, *Arhgdib*, and *Cdc42* were as follows:

β-actin, F:TGGCACCCAGCACAATGAA and R: CTAAGTCATAGTCCGCCTAGAAGCA;

Cdc42, F: GGCTGTCAAGTATGTGGAGTGTTTC and R: CTCCAGGGCAGCCAAT;

Arhgdib, F:GGACTGGGGTGAAAGTGGATAA and R: GAGTGACAGGGTGGGAAAAGAT.

Following the manufacturer's instructions, the comparative threshold cycle method was used to analyze the data with gene expression levels calibrated to those of the housekeeping gene, *β-actin*. PCR was performed in triplicate for each specimen and three independent experiments were performed.

RESULTS

When Y-27632-treated hES cells were floated in a nonadherent dish immediately after thawing, most cells were intact and round in shape (Fig. 1). The cells adhered to each other and formed huge clusters consisting of 10–20 cells within 6 h. Untreated single hES cells did not adhere to each other and showed marked morphological changes as time elapsed. Bud-like structures, hereafter called blebs, formed on the cell surface and fused to form large swellings. These structures deconstructed and formed small fragments.

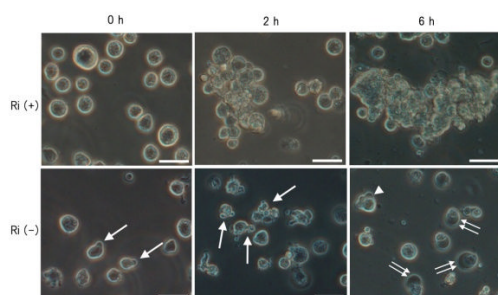


Figure 1. $R_i(+)$: Y-27632-treated hES cells after thawing. A cluster is formed at 2 h and becomes huge at 6 h. $R_i(-)$: Untreated cells do not form a cluster. Definite blebs (arrows) are recognized on the cell surface at 2 h, though hES cells begin to lose their shape immediately after thawing (at 0hr, arrows). At 6 h, blebs fuse (arrow head) and form a large swelling with no definite intracellular organelles (double arrows). Bar = 20 µm

In Y-27632-treated hES cells, E-cadherin distributed along the membrane and became more marked as cells formed clusters. It appeared in the cytoplasm at 1 h (Fig. 2), while Oct3/4 remained restricted to the nucleus. In untreated cells, E-cadherin lost its even distribution along the membrane and formed small condensed “dots” in the membrane. As time elapsed, E-cadherin displayed eccentric localization in the cytoplasm and Oct3/4 disappeared. The cells deformed and their membranes became undulated with blebs. E-cadherin appeared to be constricted to the blebs or immediately below them. The blebs then deconstructed and formed fragments with a DAPI-positive nucleus and a small section of cytoplasm, including a small amount of E-cadherin.

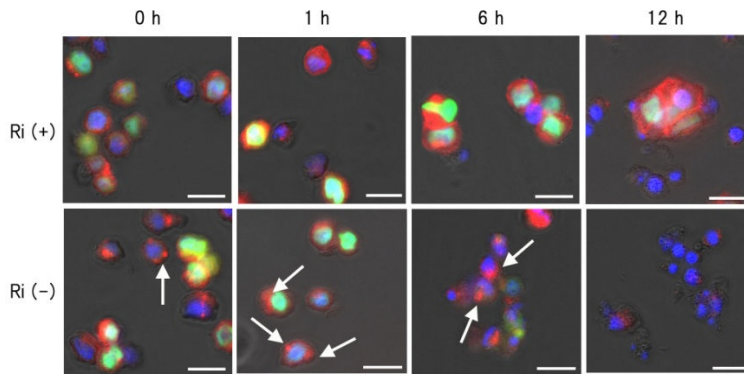


Figure 2. $R_i(+)$: E-cadherin (red) is observed along the membrane immediately after thawing (0 h) and Oct3/4 (green) is restricted to the nucleus (DAPI: blue). As hES cells cluster, E-cadherin becomes more marked along the membrane and Oct3/4 is found in the nuclei of all cells forming the cluster. $R_i(-)$: E-cadherin is dotted along the membrane at 0 h (arrow) and Oct3/4 is often lost. E-cadherin moves from the membrane into the cytoplasm, and is localized near a bleb at 1 h (arrows). It shows eccentric localization at 6 h (arrows) and subsequently, Oct3/4 disappears. At 12 h only fragments with a tiny DAPI-positive nucleus

F-actin distributed as a fine network under both conditions immediately after thawing, although red fluorescence was intense along the membrane (Fig. 3). The F-actin network appeared to be condensed in the cytoplasm of treated cells at 1 h, but soon expanded into the

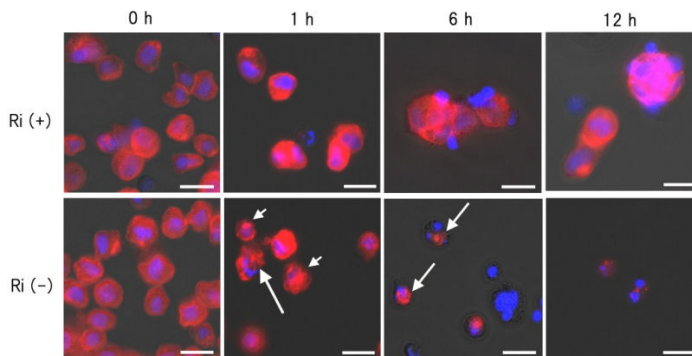


Figure 3. F-actin (red) distribution: F-actin forms a fine network in the cytoplasm under both conditions immediately after thawing. This fine network is maintained in $R_i(+)$ cells in which hES cells form clusters. However, it condenses in the cytoplasm near the blebs (but not in them) at 1 h in $R_i(-)$ cells (long arrow). Blebs look pale because of loss of F-actin (short arrows). As time elapses, there is less condensation at 6 h (arrows) and eventually it disappears at 12hr altogether. DAPI (blue) Bar = 20 μ m

cytoplasm as hES cells formed clusters. In untreated cells, F-actin showed marked condensation in the cytoplasm at 1 h. The condensation was close to the blebs but not inside them. Blebs were poorly stained because F-actin was lost. As time elapsed, F-actin condensation was accelerated, and eventually, the fine network disappeared.

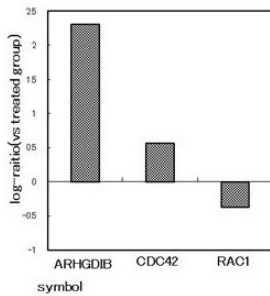


Figure 4. Microarray screening of G13 pathway at 12 h after thawing. Y-axis shows the experimental sample [R_i(-)] versus the reference sample [R_i(+)] log-ratio. *Arhgdib* is markedly upregulated and *Cdc42* increases moderately, but *Rac1* is downregulated.

The G13 signaling pathway is closely associated with actin reorganization (2, 3) and in this study, changes in some components associated with this pathway were confirmed by DNA microarray. Upregulation of *Arhgdib* and *Cdc42* and downregulation of *Rac1* was observed in untreated cells 12 h after thawing (Fig. 4). Quantitative PCR confirmed that the expression of *Cdc42* and *Arhgdib* increased in untreated [R_i(-)] hES cells compared to that in treated [R_i(+)] cells (Fig. 5).

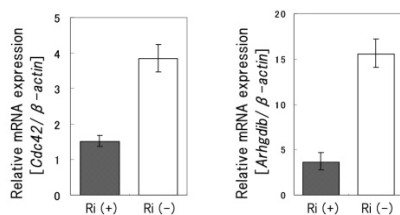


Figure 5. *Cdc42* and *Arhgdib* are upregulated 12 h after thawing. *Cdc42* expression in R_i(-) is about three times of that seen in R_i(+). *Arhgdib* is approximately four times of that seen in R_i(+) cells.

DISCUSSION

A number of studies (6, 21), including one of our own (under submission), have shown that apoptosis plays a major role in cell death via the caspase family enzymes after freeze-thawing. However, as mentioned in the present study, a pathway, other than the apoptotic

pathway, to cell death exists. This pathway is characterized by poor cell–cell adhesion, abnormal localization of E-cadherin in the cytoplasm, and uneven condensation of F-actin. After thawing, blebs or cytoplasmic protrusions were formed in untreated hES cells; these contain no intracellular organelles and are amorphous in structure. Although the boundary line is not definite, blebs are demarcated by the cytoplasm. E-cadherin moves from the membrane through the blebs and accumulates in the cytoplasm near the blebs. F-actin tends to condense in the cytoplasm near the blebs. Blebs fuse with each other around the neck region and may rupture. These findings suggest that disruption of the intimate interrelationship between actin filaments and E-cadherin is associated with cell death.

The G13 signaling pathway is important for understanding these processes because it is activated by G13, a subunit of the heterotrimeric guanine nucleotide–binding proteins (G proteins) that route the signals to several distinct intracellular signaling pathways and regulate actin cytoskeletal remodeling (13, 16). Therefore, we used DNA microarray to investigate a few components associated with this pathway. Among a large number of candidates, definite upregulation of *Arhgdib* and *Cdc42* was observed in Y-27632-untreated hES cells than in treated hES cells. This observation was confirmed by quantitative PCR.

Many reports have suggested that *Cdc42* directly affects actin remodeling and functioning (4, 17). *Arhgdib* is a G13 signaling pathway component that when activated stimulates *Cdc* and *Rac* (5). *Rac* was shown to be nonfunctional in thawed single hES cells in this study. *Cdc* plays a major role in disrupting the actin-cytoskeletal network. Although our study makes it clear that the G13 signaling pathway is important for understanding the biological processes that occur in hES cells during freeze-thawing, it remains unclear why the cells do not adhere to each other and why cell death occurs via this pathway. This pathway is associated with intercellular junctions, especially adherence junctions, because adherence junctions are constructed by cadherins and are directly affected by cytoplasmic actin filaments via anchor proteins such as catenin (15). hES cells express E-cadherin more markedly than other undifferentiated cells like ectoderm or mesoderm, with a relatively homogenous distribution (11). Furthermore, a higher E-cadherin level is suggested to be associated with a higher likelihood of cell agglomeration and subsequent survival in suspension (18). In our study, Y-27632-treated hES cells, which maintained their E-cadherin level, rapidly formed clusters comprising several cells before proliferation and were revived along with rapid recovery of nuclei function. However, untreated hES cells did not agglomerate and did not survive. E-cadherin displayed eccentric localization in the cytoplasm, and the cells basically did not have any way to adhere to each other. Furthermore, Oct3/4 proteins disappeared with the abnormal distribution of E-cadherin and were not recovered. According to Popoff and Geny (17), *Rac/Cdc42* coordinate the assembly–disassembly of adherence junction components. Moreover, a subtle balance and interplay between Rho/Ras-GTPase activity is required to maintain optimal organization and function of junctions. Lin et al. (12) proved that epiboly (cell movement in the early embryo) in the zebrafish was regulated by G α (12/13), partly by the association with the cytoplasmic terminus of E-cadherin, thereby inhibiting E-cadherin activity and cell adhesion. They demonstrated that G α (12/13) modulates epibolic movements in the cell envelope layer by regulating actin cytoskeleton organization through a RhoGEF/Rho-dependent pathway. Considering these reports and the findings in this study, we believe that hyperactivation of the G13 signaling pathway after thawing disturbs the functional balance between actin cytoskeleton and E-cadherin distribution, disrupts the cell shape, inhibits cell–cell adhesion, and prevents the establishment of cell cooperation, leading to the death of individual hES cells. This cell death pathway can be partly suppressed by the ROCK inhibitor. These results are summarized in Fig. 6.

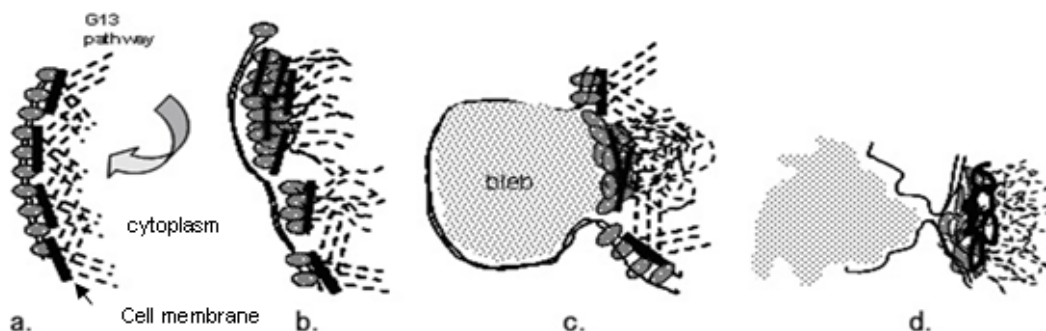


Figure 6. Schematic diagram of bleb formation and rupture in untreated single hES cells induced by disruption of the E-cadherin–actin filament network via the G13 signaling pathway after thawing. **(a)** The G13 signaling pathway components *Arhgdib* and *Cdc42* disrupt the actin filaments. **(b)** E-cadherin moves into the cytoplasm from the membrane and actin filaments are disrupted. Aggregations appearing as small “dots” form near the cell surface, and the cell membrane undulates and swells, forming blebs. **(c)** A huge bleb develops and is demarcated from the cytoplasm by aggregation of E-cadherin, actin filaments, and anchor proteins. **(d)** The bleb ruptures as its base (neck) is squeezed, probably due to acto-myosin contraction. ●:E-cadherin; —:anchor protein; - - - - - : actin filament

The final question is whether these cellular processes are peculiar to cryopreservation. In fact, the same processes are observed after dissociation (1). But many reports have suggested that cryopreservation and thawing themselves bring about cell death. In 2005, when hES cells were frozen as colonies, Heng et al. (6) found that if they survived, hES cells agglomerated with time. In 2008, Li et al. (10) did not cryopreserve single hES cells, but cell clumps using Y-27632; they also found that Y-27632 was effective in maintaining viability. Even if it is not used during dissociation and freezing, and if the culture medium contains Y-27632 after thawing, survival and colony formation of hES cells improves. There is little difference in some components of the G13 signaling pathway following dissociation between 10 μ M of Y-27632 in the cryoprotection solution and post-thaw medium and 10 μ M of Y-27632 in the post-thaw medium alone (unpublished data). Freeze-thawing may stimulate this pathway.

Apoptosis is not the sole cause of cell death after freeze-thawing, and should be considered when studying cell death processes.

Acknowledgements: We thank Mr. Ken Matsumoto, Nissui Pharmaceutical Co., for providing the culture medium. We also thank Mr. Susumu Ito, Ms. Kayo Suzuki, and Dr. Kiyokazu Kametani, Research Center for Instrumental Analysis, Shinshu University, for their excellent technical assistance.

REFERENCES

1. Chen G, Hou Z, Gulbranson DR & Thomson JA (2010) *Cell Stem Cell* **7**, 240-248.
2. Dahlquist KD, Salomonis N, Vranizan K, Lawlor SC & Conklin BR (2002) *Nat Genet* **31**, 19-20.
3. Doniger SW, Salomonis N, Dahlquist KD, Vranizan K, Lawlor SC & Conklin BR (2003) *Genome Biol* **4**, R7.
4. Gerthoffer WT (2005) *Can J Physiol Pharmacol* **83**, 851-856.
5. Gorvel JP, Chang TC, Boretto J, Azuma T & Chavrier P (1998) *FEBS Lett* **422**, 269-273.
6. Heng BC, Kuleshova LL, Besled SM, Liu H & Cao T (2005) *Biotechnol Appl Biochem* **41**, 97-104.
7. Heng BC, Ye CP, Liu H, Toh WS, Rufaihah AJ, Yang Z, Bay BH, Ge Z, Ouyang HW, Lee EH & Cao T (2006)[javascript:AL_get\(this, 'jour', 'J Biomed Sci.'\);](#) *J Biomed Sci* **13**, 433-445.
8. Ichikawa H, No H, Takei S, Takashimizu I, Yue F, Cui L, Ogiwara N, Johkura K, Nishimoto Y & Sasaki K (2007) *Cryobiology* **54**, 290-293.
9. Li X, Krawetz R, Liu S, Meng G, & Rancourt DE (2009) *Hum Reprod* **24**, 580-589.
10. Li X, Meng G, Krawetz R, Liu S & Rancourt DE (2008)[javascript:AL_get\(this, 'jour', 'Stem Cells Dev.'\);](#) *Stem Cells Dev* **17**, 1079-1085.
11. Li Z, Qiu D, Sridharan I, Qian X, Zhang H, Zhang C & Wang R (2010) *J Phys Chem B* **114**, 2894-2900.
12. Lin F, Chen S, Sepich DS, Panizzi JR, Clendenon SG, Marrs JA, Hamm HE, & Solnica-Krezel L (2009) *J Cell Biol* **184**, 909-921.
13. Maekawa M, Ishizaki T, Boku S, Watanabe N, Fujita A, Iwamatsu A, Obinata T, Ohashi K, Mizuno K & Narumiya S (1999) *Science* **285**, 895-898.
14. Martin-Ibañez R, Unger C, Strömberg A, Baker D, Canals JM & Hovatta O (2008) *Hum Reprod* **23**, 2744-2754.
15. Mège RM, Gavard J & Lambert M (2006) *Curr Opin Cell Biol* **18**, 541-548.
16. Neves SR, Ram PT & Iyengar R (2002) *Science* **296**, 1636-1639.
17. Popoff MR & Geny B (2009) *Biochim Biophys Acta* **1788**, 797-812.
18. Singh H, Mok P, Balakrishnan T, Rahmat SN & Zweigerdt R (2010) *Stem Cell Res* **4**, 165-179.
19. Suemori H, Yasuchika K, Hasegawa K, Fujioka T, Tsuneyoshi N & Nakatsuji N (2006) *Biochem Biophys Res Commun* **345**, 926-932.
20. Udy GB & Evans MJ (1994) *Biotechniques* **17**, 887-894.
21. Xu X, Cowley S, Flaim CJ, James W, Seymour L & Cui Z (2010) *Biotechnol Prog* **26**, 827-837.
22. Yamamoto Y, Banas A, Murata S, Ishikawa M, Lim CR, Teratani T, Hatada I, Matsubara K, Kato T, & Ochiya T (2008) *FEBS J* **275**, 1260-1273.
23. Watanabe K, Ueno M, Kamiya D, Nishiyama A, Matsumura M, Wataya T, Takahashi JB, Nishikawa S, Nishikawa S, Mugeruma K & Sasai Y (2007) *Nat Biotechnol* **25**, 681-686.

Accepted for publication 20/07/2011